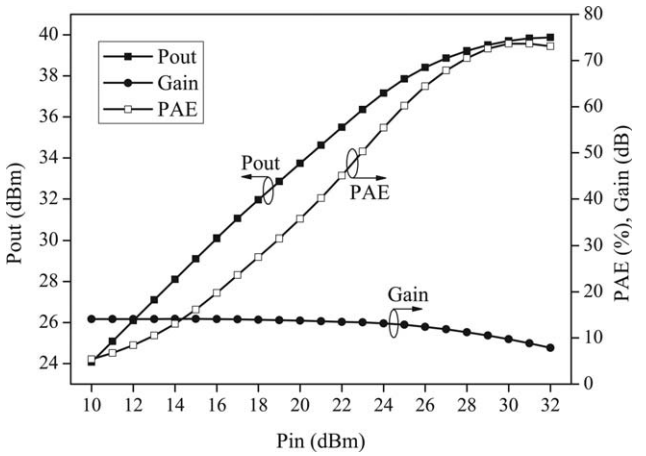

Figure 6 Measured PA performance against input power at 2.4 GHz

DBPA shows better performance at the two bands simultaneously compared with the prior works.

4. CONCLUSION

In this article, a novel and simple concurrent DB matching technique is proposed. By combining a traditional single-band MN with a DSL-based network in cascade, the impedance matching can be realized simultaneously at two distinct bands. The fabricated DBPA achieves almost same performance at the two bands. The proposed DB matching technique could be easily extended to the concurrent triband and even MB applications by adding a triband/MB DSL-based network to the right side of the proposed DBMN.

ACKNOWLEDGMENT

This work was supported by the National Science and Technology Major Project of China (Contract No. 2012ZX03004008).

REFERENCES

1. M. Steer, Beyond 3G, IEEE Microwave Mag 8 (2007), 76–82.
2. E. McCune, High-efficiency, multi-mode, multi-band terminal power amplifier, IEEE Microwave Mag 6 (2005), 44–55.
3. G. Nikandish, E. Babakrpur, and A. Medi, A harmonic termination technique for single- and multi-band high-efficiency class-F MMIC power amplifiers, IEEE Trans Microwave Theory Tech 62 (2014), 1212–1220.
4. K. Chen, T.C. Lee, and D. Peroulis, Co-design of multi-band high-efficiency power amplifier and three-pole high-Q tunable filter, IEEE Microwave Wireless Compon Lett 23 (2013), 647–649.
5. R. Negra, A. Sadeve, S. Bensmida, and F.M. Ghannouchi, Concurrent dual-band class-F load coupling network for applications at 1.7 and 2.14 GHz, IEEE Trans Circuits Syst 55 (2008), 259–263.
6. P. Colantonio, F. Giannini, R. Giofre, and L. Piazzon, Dual band power amplifier in GaN technology, Microwave Opt Technol Lett 50 (2008), 1040–1042.
7. K. Rawat and F.M. Ghannouchi, Dual-band matching technique based on dual-characteristic impedance transformers for dual-band power amplifiers design, IET Microwave Antennas Propag 5 (2011), 1720–1729.
8. P. Chen, S. He, X. Wang, and Z. Dai, 1.7/2.6 GHz high-efficiency concurrent dual-band power amplifier with dual-band harmonic wave controlled transformer, Electron Lett 50 (2014), 184–185.
9. J. Li, Y. Liu, S. Li, C. Yu, and Y. Wu, Design of dual-band phase offset line with arbitrary phase shift at two operational frequencies, Electron Lett 50 (2014), 91–93.

ENHANCEMENT IMPEDANCE TRANSFORMING RATIOS OF COUPLED LINE IMPEDANCE TRANSFORMER WITH WIDE OUT-OF-BAND SUPPRESSION CHARACTERISTICS

Phirun Kim, Girdhari Chaudhary, and Yongchae Jeong
Division of Electronics and Information Engineering, IT convergence Research Center, Chonbuk National University, Jeonju, Republic of Korea; Corresponding author: ycjeong@jbnu.ac.kr

Received 2 January 2015

ABSTRACT: *This article presents the design of an impedance transformer (IT) with wide out-of-band suppression characteristics. The wide out-of-band suppression characteristics can be obtained by loading several transmission zeros in the lower and upper out-of-bands. For experimental validation, a 50-to-10 Ω IT was implemented at a center frequency (f_0) of 2.6 GHz for the long term evolution signal. The measured results are in good agreement with the simulations, showing a return loss higher than 20 dB over a passband bandwidth of 0.35 GHz (2.35–2.7 GHz) and out-of-band suppression better than 18 dB from DC to 1.78 GHz and from 3.45 to 6.97 GHz.* © 2015 Wiley Periodicals, Inc. Microwave Opt Technol Lett 57:1600–1603, 2015; View this article online at wileyonlinelibrary.com. DOI 10.1002/mop.29144

Key words: *coupled line; transmission zeros; wide out-of-band impedance transformer*

1. INTRODUCTION

The impedance transformer (IT) is one of the key circuits in microwave systems. It transforms a termination impedance to an arbitrary impedance and has been implemented for many applications, such as power divider [1], antenna [2], and matching circuits in filters [3,4]. In [5], an open-circuited coupled line IT, which can act as a DC block, was presented. It can provide matching characteristics in the passband (f_0) and a transmission zero in the second harmonic band ($2f_0$) only. Similarly, a multiconductor coupled structure was proposed in [6] and a coupled line IT, in which the coupled port was connected back to the input port, was presented in [7]. However, these works were focused on the passband matching characteristics and did not consider the out-of-band suppression characteristics. An IT using a lumped equivalent circuit of left-handed transmission line (TL) section with an impedance transforming ratio (r) of 2 was mentioned in [8]. Moreover, this network provided perfect matching performance at f_0 and did not consider the out-of-band suppression characteristics. If a bandpass filtering IT can be realized, the burdens of the filter such as the insertion loss and out-of-band suppression can be reduced, which is a critical design issue in the case of a high power amplifier design. In [9], a coupled line IT was presented with good out-of-band suppression. However, r is low and the out-of-band suppression is not sufficient.

In this article, a design method for an IT with wide out-of-band suppression characteristics is presented based on a parallel coupled line and a shunt open TL. The high impedance transforming ratio (HITR) and out-of-band suppression are enhanced by modifying the stub position compared with [9]. To verify the proposed IT network, a 50-to-10 Ω IT was designed, simulated, and fabricated at the f_0 of 2.6 GHz.

2. DESIGN EQUATION

Figure 1 shows the proposed IT structure. It is composed of a parallel coupled line with odd- and even-mode impedances (Z_{0o}

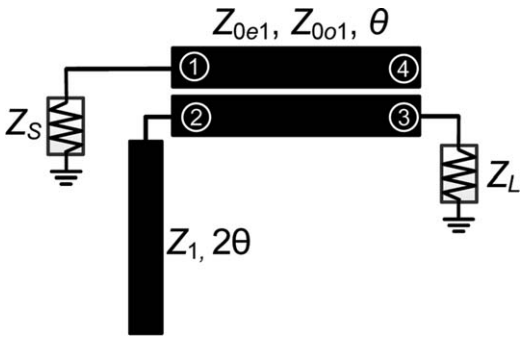

Figure 1 Block diagram of proposed IT

and Z_{0e}) and a shunt open stub TL with a characteristic impedance of Z_1 connected at coupling Port 2. The electrical lengths of the coupled line (θ) and the shunt open stub TL (2θ) are given as the quarter-wavelength ($\lambda/4$) and half-wavelength ($\lambda/2$) at f_0, respectively. As shown in Figure 1, the load impedance (Z_L) can be transformed to the source impedance (Z_S) by controlling Z_{0o} and Z_{0e} of the coupled line. Moreover, the shunt open stub TL is used to create passband transmission poles as well as two transmission zeros, which are located at the lower and upper sides of the passband, respectively.

The reflection and transmission coefficients of the proposed IT network, where input Port 1 and output Port 3 are terminated with impedances Z_S and Z_L, respectively, can be derived from [10], as shown in Eqs. (1) and (2).

$$S_{11} = \frac{(Z_{11}-Z_S)(Z_{22}+rZ_S)-Z_{12}Z_{21}}{(Z_{11}+Z_S)(Z_{22}+rZ_S)-Z_{12}Z_{21}} \tag{1a}$$

$$S_{21} = \frac{2Z_{21}Z_S\sqrt{r}}{(Z_{11}+Z_s)(Z_{22}+rZ_S)-Z_{12}Z_{21}} \tag{1b}$$

where

$$Z_{11} = j\frac{\cot\theta}{2}\left(\frac{Z_m^2\cot\theta}{2Z_1\cot 2\theta+Z_p\cot\theta}-Z_p\right) \tag{2a}$$

$$Z_{22} = j\frac{Z_p}{2}\left(\frac{Z_p\csc^2\theta}{2Z_1\cot 2\theta+Z_p\cot\theta}-\cot\theta\right) \tag{2b}$$

$$Z_{21} = Z_{12} = j\frac{Z_m}{2}\csc\theta\left(\frac{Z_p\cot\theta}{2Z_1\cot 2\theta+Z_p\cot\theta}-1\right) \tag{2c}$$

$$\theta = \frac{\pi}{2}\frac{f}{f_0} \tag{2d}$$

$$Z_p = Z_{0e}+Z_{0o} \tag{2e}$$

$$Z_m = Z_{0e}-Z_{0o} \tag{2f}$$

At f_0, the reflection and transmission coefficients can be obtained as shown in Eqs. (3a) and (3b), respectively.

$$S_{11}|_{f=f_0} = \frac{Z_m^2-4rZ_S^2}{Z_m^2+4rZ_S^2} \tag{3a}$$

$$S_{21}|_{f=f_0} = \frac{-j4Z_mZ_S\sqrt{r}}{4rZ_S^2+Z_m^2} \tag{3b}$$

As seen from Eqs. (3a) and (3b), the reflection and transmission coefficients only depend on Z_{0e} and Z_{0o} of the coupled line, and are independent of Z_1.

Figure 2 shows the reflection coefficient characteristics at f_0 according to Z_{0e} in the cases of $Z_{0o} = 40\ \Omega$, $Z_L = 50\ \Omega$, and $Z_S = (16.66,\ 10,\ \text{and}\ 5\ \Omega)$ (or $r = 3,\ 5,\ \text{and}\ 10$). From this figure, it is categorized into three different regions [9], depending on Z_{0e}, which can be described by (4).

$$(Z_{0e}-Z_{0o}) < 2Z_s\sqrt{r}\ : \text{under-matched} \tag{4a}$$

$$(Z_{0e}-Z_{0o}) > 2Z_s\sqrt{r}\ : \text{over-matched} \tag{4b}$$

$$(Z_{0e}-Z_{0o}) = 2Z_s\sqrt{r}\ : \text{perfectly-matched} \tag{4c}$$

The value of Z_{0e} with specified values of S_{11}, Z_S, and r at f_0 can be found from Eq. (3a) for an under-matched region as shown in Eq. (5).

$$Z_{0e} = 2Z_S\sqrt{\frac{r\left(1-S_{11}|_{f=f_0}\right)}{1+S_{11}|_{f=f_0}}}+Z_{0o} \tag{2}$$

Similarly, the value of Z_{0e} for an over-matched region can be found from Eq. (3a) and condition (4b), as shown in Eq. (6).

$$Z_{0e} = 2Z_S\sqrt{\frac{r\left(1+S_{11}|_{f=f_0}\right)}{1-S_{11}|_{f=f_0}}}+Z_{0o} \tag{3}$$

In a perfectly-matched region, S_{11} becomes zero, so that the value of Z_{0e} can be found as shown in Eq. (7).

$$Z_{0e} = 2Z_S\sqrt{r}+Z_{0o} \tag{4}$$

From Eqs. (5), (6), and (7), the coupling coefficient (C) of the different matched regions is given by Eq. (8).

$$C = \frac{Z_{0e}-Z_{0o}}{Z_{0e}+Z_{0o}}. \tag{5}$$

In addition, the characteristic impedance Z_1 is calculated to provide transmission poles in the passband and transmission zeros in the out-of-band. From (1a), Z_1 can be obtained by setting $S_{11} = 0$ as shown in Eq. (9).

$$Z_1 = \frac{Z_{0e}+Z_{0o}}{r-1} \tag{6}$$

As seen in Eq. (9), r should be higher than 1.

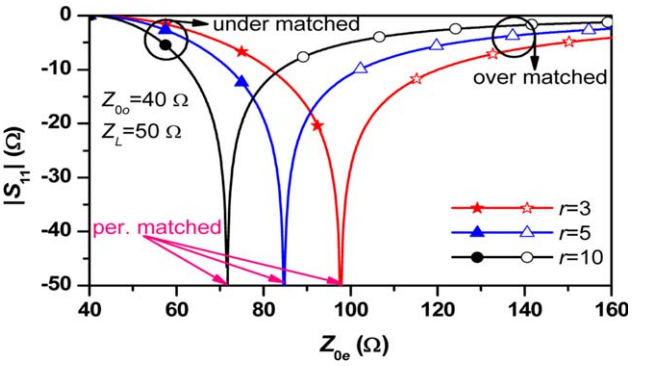

Figure 2 Reflection coefficient characteristics at center frequency according to Z_{0e} with different values of r. [Color figure can be viewed in the online issue, which is available at wileyonlinelibrary.com]

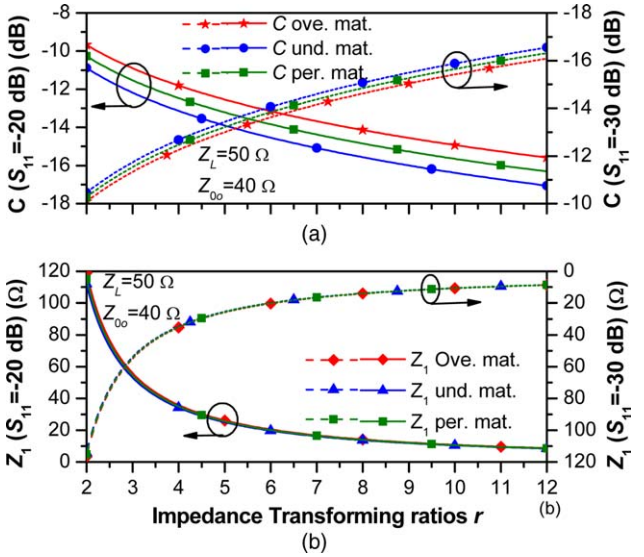

Figure 3 Calculated values according to r for: (a) coupling coefficient and (b) characteristic impedance Z_1. [Color figure can be viewed in the online issue, which is available at wileyonlinelibrary.com]

From Eq. (1b), the normalized transmission zero frequencies are given by Eq. (10).

$$f_{zt}/f_0 = \frac{(2n-1)}{2} \tag{10a}$$

$$f_{zc}/f_0 = 2n \tag{10b}$$

where n, f_{zt}, and f_{zc} are an integer and the transmission zero frequencies generated by the TL and coupled line, respectively. From the above equations, the relation between C of the coupled line and Z_1 of the shunt open stub TL is plotted in Figure 3 according to the value of r with different return losses. As can be seen from this figure, C and Z_1 decrease as r increases. The coupled line can be realized easily with a high r, however, it is difficult to fabricate a shunt open stub TL with microstrip line having a low characteristic impedance. Therefore, the tradeoff between r and Z_1 should be considered to design the proposed IT. The calculation is done by assuming that $Z_L = 50\ \Omega$, $Z_{0o} = 40\ \Omega$, and $S_{11} = -20, -30$ dB.

To verify the analysis, the S-parameter characteristics are shown in Figure 4 for the maximum S_{11} of -20 dB in the case of the under-, perfectly-, and over-matched regions. The calculated values of all cases are shown in Table 1. Figures 4(a) and 4(b) show the narrow and wideband frequency characteristics, respectively. As seen from these figures, the reflection coefficient characteristic with two poles is obtained only in the over-

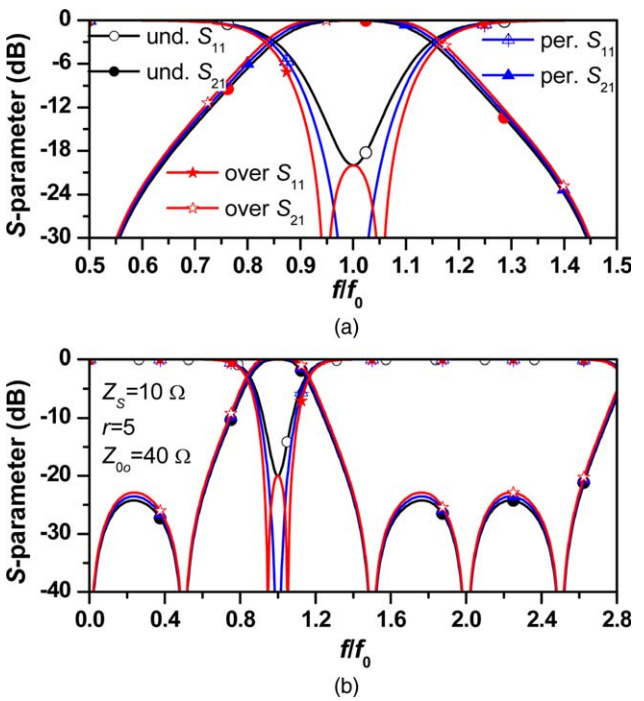

Figure 4 Frequency response for the specific matched regions: (a) narrow band and (b) wideband characteristics. [Color figure can be viewed in the online issue, which is available at wileyonlinelibrary.com]

TABLE 1 Calculated Values of the IT

Z_L=50 Ω, r=5, Z_{0o}=40 Ω, S_{11}=-20 dB			
	Under-mat.	Perf.-mat.	Over-mat.
Z_{oe} (Ω)	80.45	84.72	89.44
Z_1(Ω)	30.11	31.18	32.36

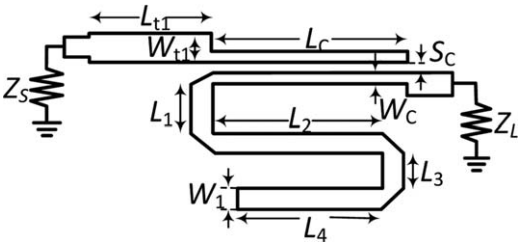

Figure 5 EM simulation layout of proposed IT

TABLE 2 Physical Dimension of the Proposed IT

W_1=2.8 mm	L_1=L_3=3.6 mm	W_{t1}=6.1 mm
Wc=1.1 mm	L_2=16 mm	L_{t1}=18.5 mm
S_c=0.25 mm	L_4=14.2 mm	L_c=21.1 mm

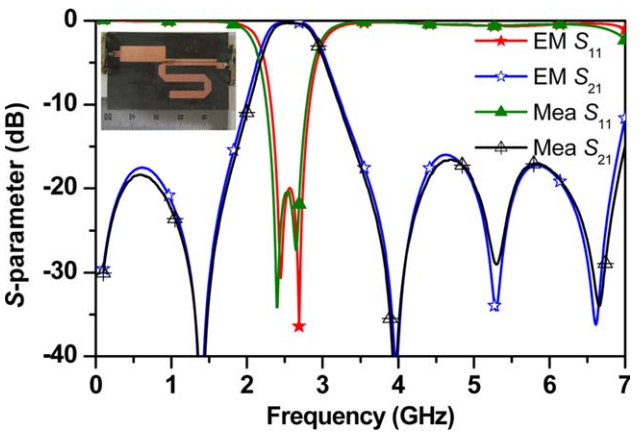

Figure 6 EM simulation and measurement of S-parameter of IT. [Color figure can be viewed in the online issue, which is available at wileyonlinelibrary.com]

TABLE 3 Performance Comparison of the Proposed IT with Previous Studies

Ref.	f_0 (GHz)	(S_{11}=−20 dB) FBW	Impedance ratio	Out-of-band suppression	PCB Technology
[5]	2	≈7%	2	NA	Microstrip Line
[7]	0.7	≈12.8%	3.4	NA	Microstrip Line
[8]	3	≈7.6%	2	NA	Microstrip Line
[9]	2.6	35.38%	2	>18 dB DC to 1.42 GHz and 3.8 to 6.65 GHz	Microstrip Line
This work	2.6	13.5%	5	>18 dB DC to 1.78 GHz and >16 dB 3.45 to 6.97 GHz	Microstrip Line

matched region, whereas a single pole characteristic is obtained in the perfectly- and under-matched regions. Therefore, the over-matched region is preferable for the widest return bandwidth characteristics. Moreover, four transmission zeros (one at the lower side and three at the upper side of the passband) are obtained in all regions, so that wide out-of-band suppression characteristics can be provided.

3. SIMULATION AND MEASUREMENT RESULTS

To experimentally validate the proposed IT network, a 50-to-10 Ω ($r = 5$) IT with maximum S_{11} of −20 dB at 2.6 GHz was designed, simulated, and measured. According to the simulation performance shown in Figure 4, the over-matched region was chosen. The calculated values are shown in Table 1. The odd-mode impedance (Z_{0o}) of the coupled line was chosen for the fabrication of the coupled line. The circuit was fabricated on an RT 5880 substrate with $\varepsilon_r = 2.2$ and $h = 31$ mil. The electromagnetic (EM) simulation was performed using HFSS v15 from Ansoft.

Figure 5 shows the EM simulation layout of the designed IT network. The physical dimensions are shown in Table 2. The $\lambda/4$ IT at the source port is used to perform the measurements with the 50 Ω termination impedance of the network analyzer. To minimize the circuit size, the $\lambda/2$ TL is designed as a meander structure. The circuit size of the proposed IT is 22.5 × 13.4 mm^2 (ignoring the quarter-wavelength IT used for the measurement).

Figure 6 shows the EM simulation, measurement results, and a photograph of the fabricated circuit. The measured results are in good agreement with the simulations. From the measured results, the return loss was determined to be 22.57 dB at $f_0 = 2.6$ GHz. Similarly, the 20 dB return loss bandwidth is 0.35 GHz (2.35–2.7 GHz). The insertion loss in the same band is smaller than 0.32 dB, including the loss of the $\lambda/4$ IT for the measurement. As seen from the measurement result, one transmission zero is obtained on the lower side of the passband and three transmission zeros on the upper side, providing wide out-of-band suppression characteristics. The $\lambda/2$ shunt open TL generates three transmission zeros at 1.4, 3.95, and 6.66 GHz, respectively. Moreover, the $\lambda/4$ coupled line generates a transmission zero at 5.3 GHz. The out-of-band signal suppression characteristic is more than 18 dB from DC to 1.78 GHz on the lower side of the passband, and is more than 16 dB from 3.45 to 6.97 GHz on the upper side of the passband. Compare with [9], the out-of-band suppression characteristics of the proposed circuit may seem worse. However, if the proposed circuit is designed with the same condition ($r = 2$), the out-of-band operation and bandwidth would be better on the simulation comparison. Therefore, the proposed IT provides sharp frequency-selective matching and wide out-of-band suppression characteristics. The wide out-of-band suppression characteristics of the proposed IT are beneficial when it is applied to frequency selective circuit designs, such as high power, high efficiency, and high linear amplifier designs. Table 3 shows the results and comparison of the proposed circuit to previous works. The proposed circuit provides better out-of-band suppression characteristics and HITR when compared with the previous works.

4. CONCLUSION

This letter presents the design of an IT with wide out-of-band suppression characteristics by controlling the even- and odd-mode impedances of the coupled line and characteristic impedance of the half-wavelength shunt open stub TL. Both the simulation and measurement results are provided to validate the proposed IT. The proposed IT is simple to design and fabricate and is also expected to be applicable in various RF circuits and systems that require frequency selective performance.

REFERENCES

1. L. Gao and X. Zhang, Novel 2:1 Wilkinson power divider integrated with banpass filter, Microwave Opt Technol Lett 50 (2013), 646–648.
2. B. Lee, F. Harackiewicz, G. Kang, U. Hong, J. Lee, and B. Kim, Enhanced impedance bandwidth of microstrip antennas using coupling, Microwave Opt Technol Lett 39 (2003), 79–81.
3. N. Karmakar and R. Ling, Compact planar bandpass filter using multisection transformers, Microwave Opt Technol Lett 43 (2004), 435–437.
4. X. Wu and Q. Chu, Hig-selectivity wideband bandpass filter using quarter-wave coupled lines and quarter-wave series transformers, Microwave Opt Technol Lett 56 (2014), 1418–1421.
5. H. Ahn and T. Itoh, Impedance-transforming symmetric and asymmetric DC blocks, IEEE Trans Microwave Theory Tech 58 (2010), 2463–2474.
6. J. Jeong, J. Kim, and S. Jeon, Tunable impedance transformer using multiconductor coupled lines, Microwave Opt Technol Lett 54 (2012), 851–853.
7. K. Ang, C. Lee, and Y. Leong, Analysis and design of coupled line impedance transformers, In: Microwave Symposium Digest, Vol. 3, Fort Worth, TX, 2004, pp. 1951–1954.
8. H. Ahn and B. Kim, Left-handed lumped transmission lines and left-handed small impedance transformers, Microwave Opt Technol Lett 50 (2008), 2269–2271.
9. P. Kim, G. Chaudhary, and Y. Jeong, Wideband impedance transformer with out-of-band suppression characteristics, Microwave Opt Technol Lett 56 (2014), 2612–2616.
10. H. Ahn, Asymmetric passive components in microwave integrated circuits, Wiley, New York, 2006.